

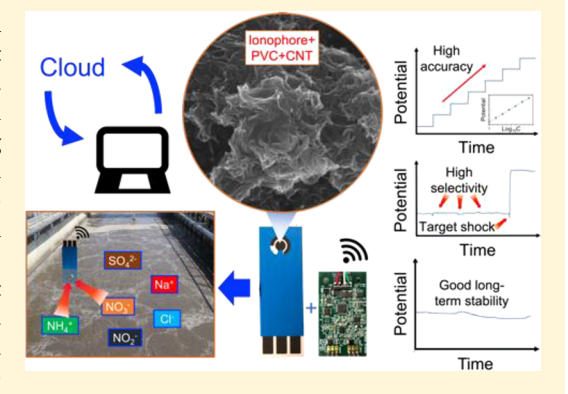
Real-Time in Situ Monitoring of Nitrogen Dynamics in Wastewater Treatment Processes using Wireless, Solid-State, and Ion-Selective **Membrane Sensors**

Yuankai Huang,[†] Tianbao Wang,[†] Zhiheng Xu,[‡] Emma Hughes,[†] Fengyu Qian,[‡] Meredith Lee,[†] Yingzheng Fan, Yu Lei, Christian Brückner, and Baikun Li*, to

†Department of Civil and Environmental Engineering, ‡Department of Electrical and Computer Engineering, §Department of Chemical and Biomolecular Engineering, and Department of Chemistry, University of Connecticut, Storrs, Connecticut 06269, United States

Supporting Information

ABSTRACT: Real-time, in situ accurate monitoring of nitrogen contaminants in wastewater over a long-term period is critical for swift feedback control, enhanced nitrogen removal efficiency, and reduced energy consumption of wastewater treatment processes. Existing nitrogen sensors suffer from high cost, low stability, and short life times, posing hurdles for their mass deployment to capture a complete picture within heterogeneous systems. Tackling this challenge, this study presents solidstate ion-selective membrane (S-ISM) nitrogen sensors for ammonium (NH₄⁺) and nitrate (NO₃⁻) in wastewater that were coupled to a wireless data transmission gateway for real-time remote data access. Lab-scale test and continuous-flow field tests using real municipal wastewater indicated that the S-ISM nitrogen sensors possessed excellent accuracy and precision, high selectivity, and multiday stability. Importantly, autocorrections of the sensor readings on the cloud minimized temperature



influences and assured accurate nitrogen concentration readings in remote-sensing applications. It was estimated that real-time, in situ monitoring using wireless S-ISM nitrogen sensors could save 25% of electric energy under normal operational conditions and reduce 22% of nitrogen discharge under shock conditions.

1. INTRODUCTION

Biological nitrogen removal (BNR) systems have suffered from long-standing problems of high energy consumption and low efficiency.1 To unlock the "black box" of BNR systems, a complete picture of the physicochemical reactions occurring in wastewater must be gained. Traditional nitrogen analytical methods are usually in passive monitoring modes, requiring water samples to be taken from wastewater treatment plants (WWTPs) to laboratories for analyses; many are complicated, tedious, or costly. Most importantly, there is an inherent significant time lag between the change of the nitrogen status and the resulting intervention. ²⁻⁴ Real-time in situ nitrogen sensors, such as ZnO nanorod-based field-effect transistor ammonium sensors,⁵ received interest, but these sensors can only measure single parameters (e.g., ammonium or nitrate) at a single point,6 making it difficult to capture a whole picture within all components of a heterogeneous wastewater system. Furthermore, most of the commercial sensors are made of costly (~\$1000 each sensor) and fragile ion-selective membranes (ISM) of low stability and short lifetime (hours to days), necessitating their frequent replacement.

A new generation of millimeter-sized (mm-sized) solid-state sensors with solid-state ion-selective membranes (S-ISM) printed on polyimide films using precision inkjet printing technology (IPT) are expected to be suitable to tackle this critical shortcoming of the established systems.^{8,9} The mmsized solid-state sensors possess distinct advantages that include easy and rapid fabrication (less than 2 h), long durability (over several weeks in wastewater), high accuracy (error less than 5%), low costs (less than \$1 each), and they have a thin structure (less than 1 mm thickness), leading to rapid responses. 10,11 We are not aware of the development of S-ISM-type nitrogen sensors currently.

Wireless remote data access is critical to monitor wastewater systems in a real-time mode. 12 For example, sudden variation of nitrogen concentrations in wastewater can cause fluctuations in system operation, possibly lead to irreversible collapse. 13 Real-time, in situ monitoring of the occurrence of shocks through remote data access enables the possibility for swift control measures that enhance the resilience of WWTPs. 14 However, existing nitrogen sensors relying on memory cards

November 27, 2018 Received: Revised: February 20, 2019 Accepted: February 26, 2019 Published: February 26, 2019



for data storage are limited to local nodes.¹⁵ Online water quality monitoring systems have been used for wireless data transmission, but the data will be stored in a repository and are not immediately available, making the system user-unfriendly.¹⁶

We report here the development of a new generation of S-ISM nitrogen (ammonium and nitrate) sensors coupled to a wireless data transmission gateway technology that enables critical real-time, in situ nitrogen monitoring. We delineate all steps toward this breakthrough accomplishment: The design and fabrication of mechanically stabile ammonium (NH₄⁺) and nitrate (NO₃⁻) S-ISM sensors, as well as the development of the linear models between the concentrations of NH₄⁺ and NO₃⁻ in wastewater and the potential signal output (mV). We demonstrate the major features of accuracy, precision, selectivity, and resolution of the two S-ISM nitrogen sensors. Wireless nitrogen S-ISM sensor prototypes were assembled and installed in a continuous flow chamber fed with real municipal wastewater. Their long-term accuracy and mechanical stability were examined over a 7 d period. This was the first time to examine the performance of wireless nitrogen sensors in real wastewater for such a long time. Finally, the potential energy-savings and pollution alleviation in a WWTP with the wireless nitrogen monitoring system developed at steady operations as well as under transient shock conditions were estimated.

2. MATERIALS AND METHODS

2.1. Fabrication of Solid-State Ion Selective Membrane (S-ISM) Nitrogen Sensors. *Electrode Manufacture.* The mm-sized solid-state sensors were fabricated by printing gold and silver inks onto a Kapton polyimide film (thickness: $127 \mu m$, American Durafilm Co.). Details about the gold ink and silver ink components, fabrication protocols, and sensor printing procedures were described previously 17-19 and are shown in the Supporting Information. To protect the wiring from water, the individually addressable sensors (dimension: $3.8 \text{ cm} \times 1.9 \text{ cm}$) were then inserted into a poly(lactic acid) (PLA)-based protector ($6.8 \text{ cm} \times 5.2 \text{ cm}$) made by a three-dimensional (3-D) printer (model: MakerGear M2; Figure 1a)

The sensing layers were prepared by drop coating of an ionophore polymer cocktails onto the electrodes:

 NH_4^+ lonophore Cocktail. This cocktail consisted of known ammonium ionophore I²⁰ (6.9% weight by weight, w/w; nonactin, Sigma-Aldrich), plasticizer 2-nitrophenyloctylether (NPOE, 92.4% w/w, Sigma-Aldrich, lead to a much more homogeneous distribution of ionophores in the polymer film and are expected to improve adhesion of the polymer on the electrode surface²¹), and potassium tetrakis(4-chlorophenyl)-borate (0.7% w/w, Sigma-Aldrich, served as cation exchanger). The NH₄⁺ ionophore cocktail (100 mg) was mixed with 50 mg of poly(vinyl chloride) (PVC; high molecular weight, Sigma-Aldrich, served as the matrix due to its chemical and mechanical stability¹² shown to be able to extend the lifetime of ISM electrodes in aqueous solution^{22,23}), and the components were fully dissolved in 500 μ L of tetrahydrofuran (THF, \geq 99.5%, Sigma-Aldrich, served to dissolved the S-ISM).

NO₃⁻ lonophore Cocktail. This cocktail consisted of known nitrate ionophore VI²⁴ (5.2% w/w, 9-hexadecyl-1,7,11,17-tetraoxa-2,6,12,16-tetraazacycloeicosane, Sigma-Aldrich), plasticizer dibutyl phthalate (DBP, 47.1% w/w, Sigma-Aldrich), tetraoctylammonium chloride (0.6% w/w, Sigma-Aldrich,

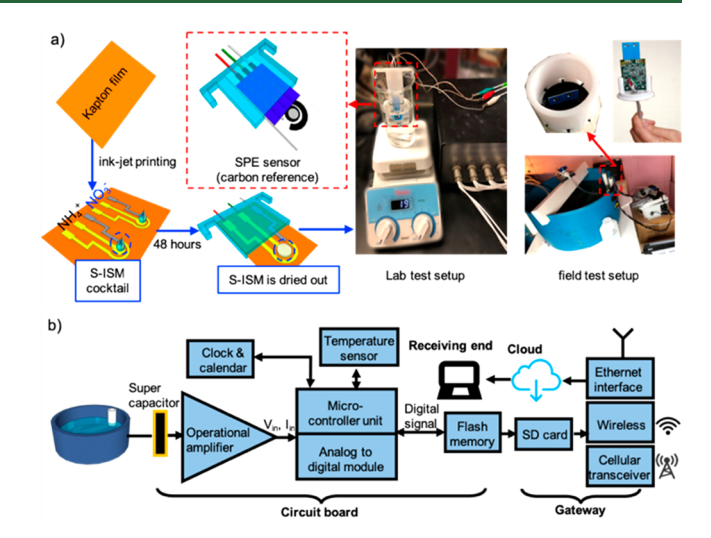


Figure 1. Diagram of the nitrogen S-ISM sensors for lab tests and field tests. (a) Fabrication process and test setup of S-ISM sensors. (b) Data transmission process of wireless nitrogen S-ISM sensors in field tests.

served as anion exchanger), and PVC (47.1% w/w, high molecular weight, Sigma-Aldrich). A portion (100 mg) of the NO_3^- ionophore cocktail was fully dissolved in 500 μL of THF.

lon-Selective S-ISM Assembly. With a micropipette, 5 μ L of each of the NH₄⁺-ionophore or NO₃⁻-ionophore cocktails were drop-cast individually onto the center of the working electrodes (diameter: 3 mm) of the solid-state electrode to form the S-ISMs (Figure 1a). After the S-ISMs were fully dried under the room temperature after 48 h, the electrodes of the NH₄⁺-specific S-ISM and NO₃⁻-specific S-ISM were soaked into 1 ppm of NH₄Cl or 100 ppm of KNO₃/MgSO₄ solutions, respectively. This conditioning process proved to be critical to reduce data drifting.²⁵

lon-Selective S-ISM_{CNT} Assembly. Prepared as described above for the ion-selective S-ISMs, but with the addition of 2% (w/w) multiwalled carbon nanotubes (CNT; 10 μm average length, 12 nm average diameter, Sigma-Aldrich, served to enhance the transfer of ions throughout the PVC and plasticizer in the S-ISM). The modified S-ISM_{CNT} sensors were compared side-by-side with the corresponding S-ISM nitrogen sensors by running an open-circuit potential-time (OCP-T) program during a 7 d lab test.

2.2. Calibration and Temperature Compensation for S-ISM Nitrogen Sensors. The $\mathrm{NH_4}^+$ - and $\mathrm{NO_3}^-$ -specific S-ISM sensors were submerged into the test solutions (100 mL) of 1 mg N/L (NH₄)₂SO₄ (0.07 M) and 1 mg N/L KNO₃ (0.07 M), respectively, and, while stirring (at 80 rpm, Thermolyne Cimarec-top stirring plate), the solutions were sequentially changed to 2, 4, 8, 16, 32, and 64 mg N/L every 30 s (Figure 1a). The readings (mV) of the $\mathrm{NH_4}^+$ and $\mathrm{NO_3}^-$ S-ISM sensors were individually recorded at an interval of 0.5 s using a CHI 660D potentiostat. The detection limit (sensitivity) of the S-ISM sensors were determined by starting with the nitrogen concentration of 1 × 10⁻⁷ M, followed by recording the potential readings in high concentration (50, 100, 200, 400, 800, and 1600 mg N/L).

The temperature compensation tests were performed by calibrating the $\mathrm{NH_4}^+$ and $\mathrm{NO_3}^-$ S-ISM sensors in solutions at 4, 12, 20, 28, and 36 °C (as per Orion 3-star conductivity

sensor, Thermo Scientific), thus quantifying the temperature impact on the slopes of calibration curves. After the temperature compensation equation was established, the S-ISM sensors were submerged sequentially into the 50 mg N/L solutions at 5, 10, 15, 20, and 25 °C to validate the concentration readings. The potential readings of NH₄⁺ and NO₃⁻ S-ISM sensors in 20 mg N/L solutions from pH 4 to pH 8 were also recorded to examine the pH interference to the sensors.

2.3. Characterization Tests of S-ISM Nitrogen **Sensors.** For the precision and accuracy test, five NH₄⁺and NO₃-specific S-ISMs were fabricated in the same batch were examined, in triplicate, along with a commercial nitrogen sensor (Professional Plus Multiparameter Instrument equipped with ammonium and nitrate probes, YSI Co.) at 5, 10, 15, 20, 25 mg N/L each, at ambient temperature (20 °C). ANOVA tests were applied to determine the significance of the reading difference among five pieces of the S-ISM sensors of the same type, while a t-test was performed to qualify the significance of the reading differences between the S-ISM sensors and commercial sensors.

For the resolution test, the NH₄⁺ S-ISM sensors and NO₃⁻ S-ISM sensors were individually examined in aqueous (NH₄)₂SO₄ and KNO₃ solutions. Their N concentrations were varied in increments, starting with an increment of 0.1 mg N/L (e.g., 5.0, 5.1, and 5.2 mg/L). If no relevant difference in the potential reading (mV) was detected on the OCP-T program (i.e., less than 0.1 mV), then larger N concentration increments (0.2, 0.3, and 0.4 mg N/L) were tested, until a relevant difference could be seen, to determine the resolution of the sensors.

For the selectivity test, the NH₄⁺ and NO₃⁻ S-ISM sensors were put individually in a solution containing different ions to examine whether they interfered with the sensor readings. For the selectivity test of the NH₄⁺ S-ISM sensor, solutions containing including Na+, Cl- (as NaCl), NO2- (as NaNO2), Ca^{2+} (as $CaCl_2$), SO_4^{2-} (as Na_2SO_4), NO_3^{-} (as $NaNO_3$), and NH₄⁺ (as (NH₄)₂SO₄) were introduced sequentially at concentrations of 5-50 mg/L to a solution of 5 mg N/L of $(NH_4)_2SO_4$ (47.2 mg/L). Similarly, for the selectivity test of the NO₃⁻ sensor, Na⁺, Cl⁻ (as NaCl), NO₂⁻ (as NaNO₂), Ca^{2+} (as $CaCl_2$), SO_4^{2-} (as Na_2SO_4), NH_4^{+} (as $(NH_4)_2SO_4$), and NO₃⁻ (as KNO₃) were introduced sequentially at concentration of 5-50 mg/L to a solution of 5 mg N/L KNO₃ (36.1 mg/L). Along with the individual interference test, the interference test of multiple nontarget ions was conducted by introducing these ions into the solution from 5 to 50 mg/L simultaneously. The readings of the NH₄⁺ and NO₃ S-ISM sensors before and after the introduction of ions were compared.

2.4. Electronics Assembly. The NH₄⁺ and NO₃⁻ S-ISM sensor nodes were assembled with a circuit board and a wireless gateway for the field test of 7 d continuous monitoring of nitrogen concentrations in real wastewater (Figure 1b). The core component of the circuit board is a microcontroller equipped with analog-to-digital (ADC) modules and arithmetic logic units (ALUs) that have multiple functions such as signal conversion, process, and storage. The circuit board also contains one major overvoltage fault survivor bounded with five diodes, one general-purpose rectifier, one resistance-based temperature sensor, one 4 Mbit flash memory, one operational amplifier (Op-amp) with a capacitor, and one clock and calendar unit (Figure S1). The final output is cached inside the

flash memory before being sent to the wireless gateway (Figure 1b). The wireless gateway contains three general purpose input/output (GPIO) pots to connect with the circuit board, a backup battery (for ~4 h), a portable computer (DART-6UL, Variscite Co.) with a wireless service for data processing and transmission to the cloud, a cellular transceiver, an Ethernet interface, a Secure Digital (SD) card, and a speaker (Figure

2.5. Field Test of Nitrogen S-ISM Sensors using Real **Wastewater.** The NH₄⁺ and NO₃⁻ sensor nodes were sealed in epoxy in a PVC-based housing tube (diameter: 6 cm, length: 13 cm) for waterproofing. They were submerged into the test solution in a continuous flow chamber (diameter: 59.1 cm, water volume: ~10 gallon) for the 7 d long-term test (Figure 1a). The chamber was fixed on a table (\sim 1.5 m high) in a test room (equipped with heating service) located in Massachusetts Alternative Septic System Test Center (MASSTC). The outside air temperature varied from -5 to 15 °C during the 7 d test (from March 27, 2018 to April 3, 2018). One lowconcentration shock and one high-concentration shock were introduced to the chamber to examine the accuracy of the NH₄⁺ and NO₃⁻ S-ISM sensors under drastic changes of nitrogen concentration. The sensor data were recorded and transmitted onto the cloud (Web site: https://portal. pointwatch.com/) every 30 s, so that all the sensor data of nitrogen concentration in the chamber could be accessed remotely in a real-time mode. To ensure the measurement accuracy, the NH₄⁺ and NO₃⁻ S-ISM sensors were calibrated on the first, 70th, and 160th hours during the 7 d test period.

2.6. Surface Characterization of S-ISM and S-SIM_{CNT} **Sensors using SEM and EDS.** The surface characterizations of the S-ISM and S-ISM_{CNT} nitrogen sensors on the scanning electron microscope (SEM) specimen stubs, after coated with a 10 nm gold-palladium layer (Polaron E5100 Sputter Coater), were performed using an FEI Nova NanoSEM equipped with an energy dispersive X-ray spectroscopy (EDS) Microanalysis Equipment (Oxford AZtecEnergy Microanalysis System with X-Max 80 Silicon Drift Detector). The EDS images targeting oxygen (O) showed the distribution of ionophore in the PVC matrix, while the images targeting chloride (Cl) showed the presence of PVC.

3. RESULTS AND DISCUSSION

3.1. Design and Fabrication of the Nitrogen S-ISM **Sensors.** The design of the NH₄⁺-/NO₃⁻-specific S-ISM sensors relied on the incorporation of ion-specific ionophores, here nonactin (also known as ammonium ionophore I) for $\mathrm{NH_4}^+$ and a 9-hexadecyl-1,7,11,17-tetraoxa-2,6,12,16-tetraazacycloeicosane (also known as nitrate ionophore VI) into a polymer matrix on a solid-state electrode (Figure 2a). Nonactin is a member of a family of naturally occurring macrotetrolide antibiotics. While the natural role of nonactin is in the recognition and selective binding of alkali group cations (particularly K⁺), it has a significant affinity for NH₄⁺ as well. It has been utilized in ammonium-specific electrodes. ²⁶ Carbonyl group hydrogen-bond acceptors displayed in a tetrahedral geometry within the nonactin receptor cavity are driving the recognition event to the hydrogen-bond donating ammonium ion. The tetraaza-tetraoxa macrocycle used as a NO₃ ionophore displays up to four highly polarized NH bonds as H-bond donors to the weakly coordinating trigonal planar nitrate anion. Its anion recognition activity has been well-characterized. ^{28,29} Both ionophores are commercially available.

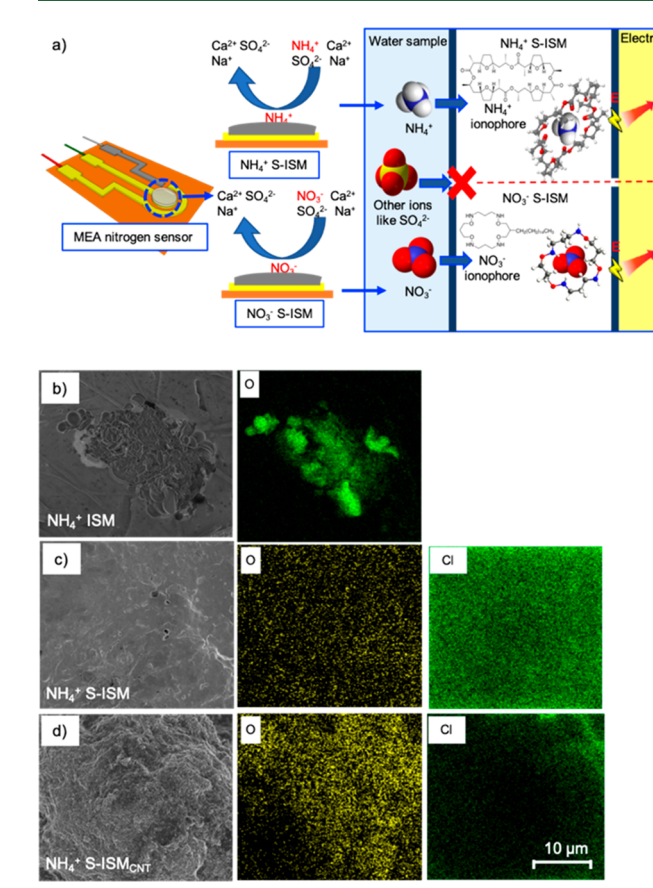


Figure 2. Structure and mechanism of the nitrogen S-ISM sensors. (a) Selectivity of the S-ISM and the dynamic steps of NH₄⁺ and NO₃⁻ ions moving from bulk water solution into S-ISM. (b) The SEM and EDS images of NH₄⁺ ISM (ionophore), atomic percentage (atom %) C: 31.02, O: 19.33. (c) The SEM and EDS images of S-ISM (ionophore mixed with PVC), atomic percentage (atom %) C: 90.19, O: 1.07, Cl: 6.03. (d) The SEM and EDS images of S-ISM_{CNT} (ionophore mixed with PVC and CNT), atomic percentage (atom %) C: 94.98, O: 3.20, Cl: 1.44. (The SEM and EDS images of NO₃⁻ S-ISM are shown in Supporting Information).

The mechanisms of S-ISM sensors rely on the specific affinity of the target ions. This affinity drives the diffusion of the analytes through the thin film. The presence of the analytes causes a change in the charge state of the electrodes, affecting its potential, thus leading to increase/decrease of its millivolt readings against an analyte-insensitive reference electrode (Figure 2a). 30,31 The rate of this change is dependent on the diffusion rate of the analytes into the matrix. Having kept the matrix thickness to less than 50 μ m, a rapid response can be anticipated.

The SEM and EDS images showed that, in the mixture of ionophore and PVC, ionophore (represented by oxygen) was evenly distributed and entrapped in the PVC compared with the dense zone crowded in the pure ionophore. The EDS image targeting chloride (Cl) showed the PVC was well-mixed in the S-ISM (Figure 2b,c for NH₄⁺ S-ISM; Figure S2a,b for NO_3^- ISM).

3.2. Calibration of Nitrogen S-ISM Sensors and **Temperature Compensation.** The calibration of NH₄⁺ and NO₃⁻ sensors was each conducted in the concentration ranges between 1 and 64 mg N/L in NH₄⁺ and NO₃⁻, the relevant concentration range of these nitrogen species in municipal wastewaters. 32,33 Both of the NH_4^+ and NO_3^- S- ISM sensors exhibited a near-Nernstian slope of 53.3 and 48.9 mV per decade of nitrogen concentration, with excellent linear regressions ($R^2 > 0.99$, Figure 3). The detection limit

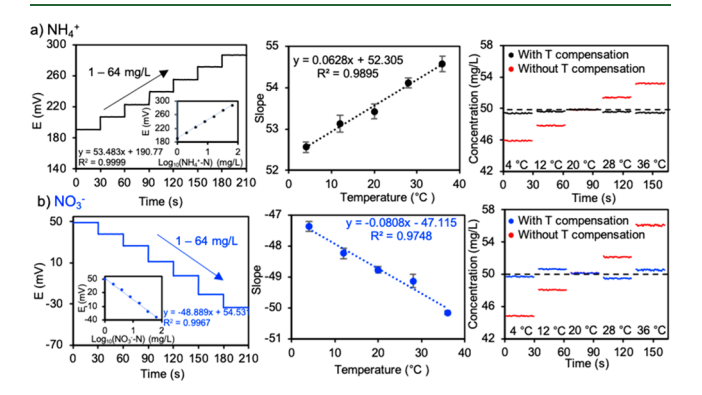


Figure 3. Calibration curves, the influence of temperature on the slope of the calibration curves, and the temperature compensation for S-ISM sensors. (a) NH₄⁺ S-ISM sensor. (b) NO₃⁻ S-ISM sensor.

(sensitivity) of NH₄⁺ and NO₃⁻ S-ISM sensor is 1 \times 10^{-6.5} M (~7.9 μg N/L) and 1 \times 10^{-5.3} M (~55.7 μg N/L), respectively (Figure S3). In the same time, both sensors showed an excellent accuracy in high nitrogen concentrations $(50-1600 \text{ mg N/L}, R^2 > 0.99, \text{ Figure S4})$. The experimental results showed comparable sensor sensitivity to previous studies. 34,35 Importantly, the sensors exhibited a prompt electrode potential (in mV) response to changes of the concentrations of NH₄⁺ and NO₃⁻, reaching steady conditions within 5 to 10 s, showing a shorter response time compared to commercial sensors (~ 10 s).

According to the Nernst equation controlling the electrode potential

$$\log_{10}(\text{analyte ion}) = \frac{(E - E^0)zF}{2.3026 \times RT}$$

it is temperature-dependent. The resulting measurement error for 50 mg N/L NH₄⁺ or 50 mg N/L NO₃⁻ for measurements between 4 and 36 °C were as large as 16.20% and 19.60%, respectively, when using the calibration curve at 20 °C (Figure 3). This large deviation necessitated a temperature compensation protocol, particularly since the temperature of wastewater in WWTPs varies on a daily and seasonal basis. Our solution to minimize the temperature error was to fabricate a mm-sized solid-state resistance-type temperature sensor¹¹ and pattern it next to the nitrogen sensor (Figure 1b, Figure S1), allowing an immediate temperature monitoring and compensation. With this compensation in place, where

$$c = 10^{\left(\frac{E - 190.96}{0.0628T + 52.305}\right)}$$

for the NH₄⁺ sensor and

$$c = 10^{\left(\frac{E - 54.531}{0.0808T + 47.155}\right)}$$

for the NO₃⁻ sensor, we were able to measure any nitrogen concentration at any temperature within the range tested, with great accuracy (Figure 3).

In contrast, a nitrogen commercial sensor (Professional Plus Multiparameter Instrument, YSI) exhibited a slow response to a temperature change (0.1 °C/sec) when a temperature shock was introduced in the lab (Figure S5), leading to a lower sensitivity and an inability for autocorrecting nitrogen readings in a real-time mode.

3.3. Precision, Accuracy, and Resolution Tests of Nitrogen S-ISM Sensors. In precision and accuracy tests, large variations of the intercepts were found for the potential readings (mV) of both the NH₄⁺ and NO₃⁻ S-ISM sensors (Figure S6). This is commonly observed for potentiometric devices.³⁶ This issue could be solved by conducting a singlepoint calibration before each usage,³⁷ since the slope of the calibration curves for a given S-ISM sensor was a fixed value (with a relative standard deviation (RSD) of less than 2% among five tests for each sensor). Two-way ANOVA analysis using the mean values of five individual sensors revealed that there was no significant difference between the readings of these five sensors (p-values higher than 0.05 for both of NH₄⁺ and NO₃⁻ sensors). The t-test results also showed that the differences between nitrogen S-ISM sensors and commercial sensors were not significant at five concentrations (Figure S7).

The resolution test showed that both of the NH₄⁺ and NO₃⁻ S-ISM sensors were able to detect increment changes of 0.1 mg N/L at low nitrogen concentration (5 mg N/L, such as wastewater effluent), with a potential (mV) difference of 0.5 mV for the NH₄⁺ sensor and 0.3 mV for the NO₃⁻ sensor. The sensors could still detect concentration increment changes of 0.2 mg/L at high nitrogen concentrations (35 mg/L, such as wastewater influent; ³² Figure S8). Summed up, the nitrogen S-ISM sensors are suited for capturing the expected nitrogen fluctuations in typical wastewater.

3.4. Sensitivity and Selectivity of S-ISM Sensors in **Wastewater.** Despite its advantages and previous use, ^{10,37,38} Ag/AgCl reference electrode is not the best electrode for most of nitrogen sensors in wastewater because of their high chloride contents (5000-10 000 mg/L³⁹), leading to measurement errors. To eliminate the chloride interference of the Ag/ AgCl reference electrode, commercial Zensor screen printed electrodes (SPEs) featuring a carbon reference electrode was used in this study (Figure 1a). The carbon electrode is remarkably stable in wastewater. 40,41 To validate this, a $\rm Cl^$ spike was injected into the test solution, increasing the Clconcentration from 5 to 50 mg/L. An obvious jump of the potential reading was observed when Ag/AgCl was used as the reference electrode, while no jump of the potential reading was observed when carbon was used as the reference electrode (Figure 4a). Similarly, the accuracy of the NH₄⁺ S-ISM sensor with a carbon-based reference electrode was examined in a NH₄Cl and (NH₄)₂SO₄ solutions, returning very similar slopes (52.06 mV/decade NH₄Cl-N and 53.34 mV/decade $(NH_4)_2SO_4-N$, respectively, at ~18 °C; Figure 4b), demonstrating the inertness (or self-compensation) of the carbon reference electrode.

Numerous ions are contained in wastewater, ⁴² posing a challenge for the selectivity of the S-ISM nitrogen sensors. Previous nitrogen sensor studies had been only conducted in pure solutions without the interference of other species. ^{43,44} The affinity and selectivity of the ionophores to their target ions is related to their complementary match of size, shape, and charge. ²⁵ Both ionophores were selected for their known affinity to the target ions (NH₄⁺ and NO₃⁻) in solution (Figure 2a). We thus conducted interference tests by sequentially adding other ions commonly found in wastewater: Na⁺, SO₄^{2-45,46} Ca²⁺ (often added to adjust pH), ⁴⁷ and NO₂⁻ (intermediate product of nitrification) ⁴⁸ into the water solution (Figure 4c,d). These nontarget ions caused nearly

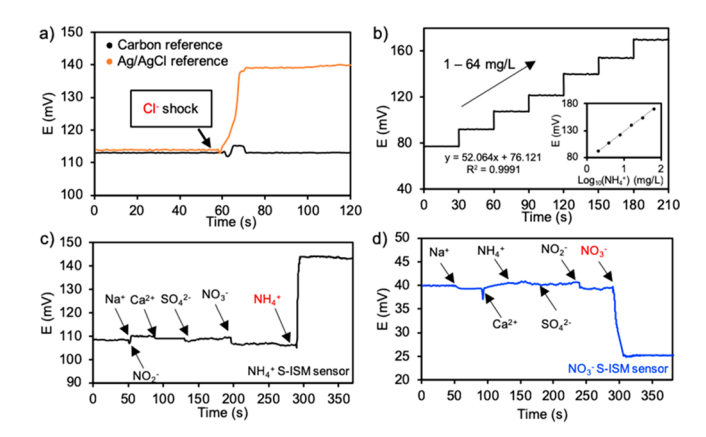


Figure 4. Selectivity tests of the nitrogen S-ISM sensors. (a) Cl^- shock results for the nitrogen sensors with a carbon reference electrode and a Ag/AgCl reference electrode. (b) The calibration curves made by NH_4^+ S-ISM sensors with carbon reference electrodes in NH_4Cl solution. (c, d) Shock tests using interference ions and targeted ions for the nitrogen S-ISM sensors.

negligible interference to the readings of both $\mathrm{NH_4}^+$ and $\mathrm{NO_3}^-$ S-ISM sensors. In contrast, when the targeted electrolytes ($\mathrm{NH_4}^+$ and $\mathrm{NO_3}^-$) were added into the solution, the sensor signals changed promptly and became stable within 15 s. Furthermore, when the interference ions were added into the solution simultaneously as the simulated wastewater, both $\mathrm{NH_4}^+$ and $\mathrm{NO_3}^-$ S-ISM sensors exhibited superior selectivity to the target electrolytes (Figure S9). This excellent selectivity over other potentially interfering ions recommended our nitrogen S-ISM sensors for the real-time, in situ monitoring of nitrogen concentrations in real wastewater.

3.5. Field Tests of Long-Term Continuous Real-Time in Situ Monitoring of Nitrogen Concentration in Real Wastewater. The accuracy and long-term stability of the S-ISM sensors were validated in field tests conducted in the MASSTC, an Environmental Protection Agency (EPA)-certified test center receiving municipal wastewater. Nitrification and denitrification systems in the MASSTC can provide effluent containing different concentrations of $\mathrm{NH_4}^+$ and $\mathrm{NO_3}^-$ to examine the sensor performance. Additionally, the wastewater temperature fluctuating daily throughout the 7 d test provided an excellent scenario to examine the accuracy of nitrogen S-ISM sensors under different temperatures.

During the 7 d continuous-flow field tests, indeed, the nitrogen sensors promptly captured two low concentration shocks (0.1 to 0.15 to 0.35 mg/L for NH_4^+ and 0.35 to 1.1 to 1.3 mg/L for NO₃⁻) and two high concentration shocks (8.3 to 22.3 to 33.8 mg/L for NH₄⁺ and 7.1 to 12.3 to 17.5 mg/L for NO₃-, Figure 5), with a discrepancy of less than 2 mg/L from the lab validation test results (Figure 6a). The minimal nitrogen detection range was 0.05 mg/L for NH₄⁺ S-ISM sensors and 0.1 mg/L for NO₃ S-ISM sensor at low concentration shocks (potential difference bigger than 0.1 mV in the raw data), showing a similar range to the lab validation tests (Figure 5 and Figure S8). The good sensitivity of the nitrogen S-ISM sensors was attributed to the effective prevention of NH₄⁺ and NO₃⁻ ionophore leakage from the PVC-based membrane (Figures 2c and S2b).⁴⁹ Furthermore, the nitrogen S-ISM sensors also promptly captured the shock incurred by feeding the treated wastewater (after nitrification) starting on the 47th hour and the shock incurred by adding raw wastewater (without any treatment) starting on the 66th **Environmental Science & Technology**

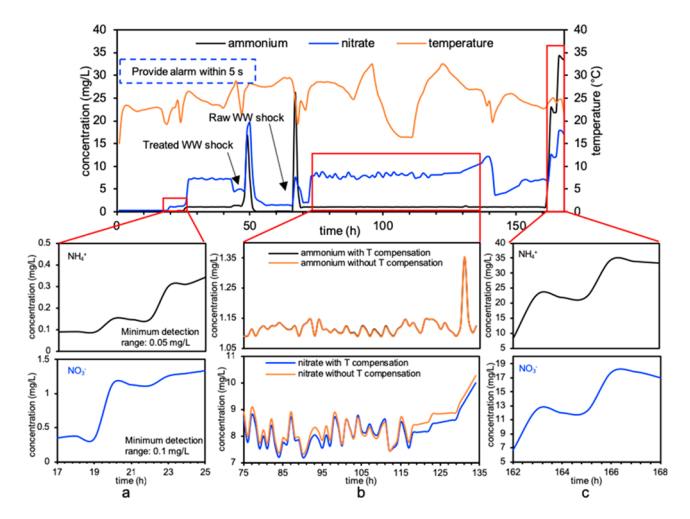


Figure 5. Readings of the nitrogen S-ISM sensors on the cloud during the 7 d continuous-flow field test using real wastewater. (a) Low-concentration shock. (b) Temperature compensation. (c) High-concentration shock.

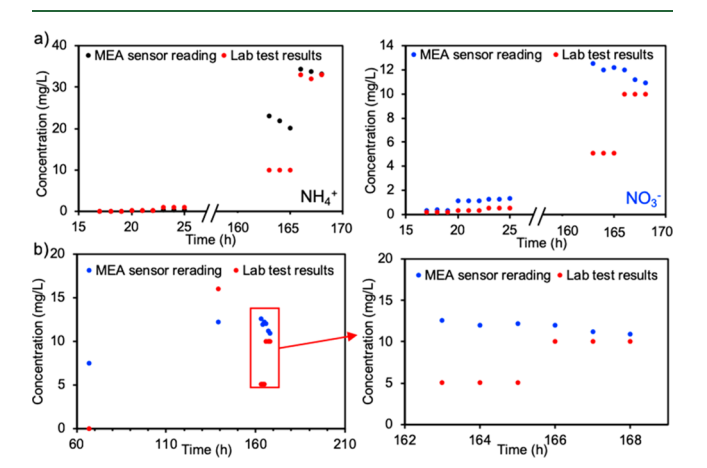


Figure 6. Comparison of the nitrogen S-ISM sensor readings and the lab validation test results during the field test. (a) Comparison of the $\mathrm{NH_4}^+$ and $\mathrm{NO_3}^-$ S-ISM sensor readings and the lab validation test results throughout the 7 d field test. (b) The comparison between the $\mathrm{NO_3}^-$ S-ISM sensor reading and the lab test results on seven tested points after 67 h in the 7 d test. The error of 4 points was higher than 5 mg N/L (67th, 164th, 165th, 166th hours).

hour. The sensor readings on the cloud provided the alarm within 5 s after the wastewater shocks (Figure 5). The interference of K^+ was negligible due to the low concentration (<1 mg/L K^+) in the field test.

However, the NO₃⁻ S-ISM nitrate sensor showed diminishing accuracy after 67 h, with the errors higher than 5 mg N/L on some points (Figure 6b). We noticed that the membrane coated on the working electrode started peeling off under the vigorous stirring in the chamber and the frequent solution change during the 7 d period (Figure S10). One conventional solution would have been to increase the ratio of PVC (e.g., from 47% w/w in this study to 60% w/w) in the NO₃⁻ ionophore for enhanced mechanical stability, but we expect that this would raise the internal resistance of the S-ISM and compromise its response behavior (Figure S11), ^{50,51} and thus this idea was rejected. Traditional liquid-state ISM sensors cannot last in the real wastewater for more than 24 h due to their friability and membrane fouling. ⁵² Some lab-scale studies

had reported that ISM sensors could last for 14 d in pure solution under static conditions (without stirring). However, this above-mentioned test scenario was completely different from the field test conducted in this study that was characterized by large chamber, vigorous mixing, frequent pumping, continuous flow, feeding solution change, chemical shock, and drastic temperature fluctuation.

Real-time capture and correction for temperature influence is a crucial challenge for in situ monitoring nitrogen concentration, especially since daily and seasonal variations of water temperature are to be expected. The resistance-type "interdigitated" temperature sensor used to capture the temperature variation exhibited a high sensitivity to temperature change (16.4 to 32.5 °C) during the 7 d test (Figure 5b and Figure S1). The real-time temperature-corrected concentration readings of the NH₄⁺ sensor was, because of the low nitrogen concentrations (1.09–1.35 mg-N/L) during this time frame, identical to those without temperature compensation. In contrast, the NO₃⁻ concentration readings showed a more stable distribution with temperature compensation (RSD: 7.7% compared to 7.91%), indicating the effect of temperature on the NO₃⁻ S-ISM sensors was diminished using the correction at relatively high nitrate concentrations (>7 mg N/L). This clearly demonstrated that the temperature correction capability of the nitrogen S-ISM sensors could ensure the accuracy of the sensor readings on the cloud. The laboratory results showed the pH also affected the sensor readings. At concentration of 20 mg N/L solution, the potential readings of NH₄⁺ and NO₃⁻ S-ISM sensors drifted from 221.6 to 250.1 mV and from -11.8 to -1.05 mV when pH increased from 4 to 8, respectively (Figure S12). However, the pH value was kept at a stable value (~6.8) during the 7 d field test, making the pH interference negligible.

After submersion in the real wastewater for 7 d in the field test, there was no obvious change on the S-ISM surface. Evidently, the judicious combination of PVC, plasticizer, and inner electrolyte components chosen led to stability and lifespan of the nitrogen S-ISM, next to its excellent the sensitivity. The latter is the result of a lowering of the zero-current ion refluxes from the S-ISM membrane into the bulk solution. However, the calibration during the field tests still showed that the readings of the NH₄+ S-ISM sensor in the 10 mg N/L NH₄+ standard solution drifted from 21 mV on Day 1 to 14.5 mV on Day 7, and the readings of the NO₃- S-ISM sensor in the 10 mg N/L NO₃- standard solution drifted from 86.5 mV on Day 1 to 66 mV on Day 7.

This "nonequilibrium" potentiometry is potentially caused by the permeability of the S-ISM membrane to oxygen and water. The lack of a redox couple between the conductive ISM and the electrode surface led to the formation of an oxygen half-cell at the inner electrode, further resulting in a concentration gradient between the bulk solution and the aqueous boundary layer adjacent to the S-ISM membrane (Figure S13).55 One possible solution to alleviate the data drifting could be mixing ionophore and PVC with carbon nanotubes (CNT) during the S-ISM fabrication process. The SEM and EDS images of the resulting S-ISM_{CNT} showed that the ionophore and PVC were entrapped onto the surface of CNT, which promoted electron transfer between the ISM and the inner electrode, enhanced transduction, and minimized the redox gradient (Figures 2d and S2c). 56,57 Indeed, lab results showed that the modified nitrogen S-ISM_{CNT} sensors lessened the data drifting to less than 30 μ V/h during the 7 d lab tests (Figure S14).

3.6. Real-Time, in Situ Monitoring, and Its Potential **Impact.** The wireless data access in the field tests showed that the signals (mV) of the nitrogen S-ISM sensors became available on the cloud within 5 s after the onset of the shocks. The combination of outstanding response and accuracy of the wireless nitrogen S-ISM sensors has the potential to greatly reduce the energy consumption for WWTPs under steady state and transient shock conditions when compared to traditional lag-time and passive manual monitoring systems that cause hour-long delays between event and response. One example may highlight the impact of a fast response time: For a WWTP with the treatment capacity of 2 million gallons per day (MGD), wireless nitrogen monitoring is expected to save ~25% of energy consumption (mainly aeration and chemical dosage) at normal steady status, as overaeration can be promptly avoided when the effluent quality requirement is met. Likewise, the real-time, wireless nitrogen monitoring system can reduce ~22% of NH₄⁺ discharge under effluent quality violation conditions (Table S1 and Figure S15).

3.7. Advantages and Future Challenges. By incorporating known ionophores in a thin polymer membrane on an electrode, we developed solid-state S-ISM nitrogen sensors with excellent sensing profiles. Coupled to wireless data transmission enabled remote data access in a real-time mode. We thus were able to monitor with high accuracy, precision, sensitivity, resolution, and stability NH₄⁺ and NO₃⁻ in wastewater remotely in real-time. This compact wireless mmsized nitrogen S-ISM sensor enables to an unprecedented degree the monitoring of nitrogen in WWTP waste streams. In fact, the wireless nitrogen S-ISM sensors could be economically friendly for both municipalities and point-of-users. It is estimated that a wastewater treatment plant with 1000 pieces of nitrogen S-ISM sensors could save more than \$1 million in terms of energy consumption and treatment efficiency (Table S2: cost analysis). For the point-of-users, disposable and durable S-ISM sensors could ease the daily water monitoring.

Note that the nitrogen S-ISM sensors suffer from the ISM-peeling off and data drifting for long-term monitoring (e.g., months). ISM mixed with poly(acrylate) of a low water diffusion coefficient and silicone rubber could reduce the water uptake in ISM⁵⁸ and might alleviate data drifting. Thereby, an S-ISM membrane with a higher hydrophobicity (e.g., poly(methyl methacrylate)—poly(decyl methacrylate) ion selective electrode (ISE) membrane, ⁵⁹ colloid-imprinted mesoporous carbon membrane ⁶⁰) will be the next step to enhance the sensor accuracy and precision.

■ ASSOCIATED CONTENT

Supporting Information

The Supporting Information is available free of charge on the ACS Publications website at DOI: 10.1021/acs.est.8b05928.

Fabrication procedures of gold ink. Fabrication procedures of sensor arrays. Details of the circuit board and the wireless gateway of the wireless S-ISM sensor assembly for 7 d field tests. Enhancement of NO_3^- ISM by mixing with PVC to form S-ISM and mixing with PVC and CNT to form S-ISM $_{\rm CNT}$. The detection limit (sensitivity) test for NH_4^+ and NO_3^- S-ISM sensors. Calibration curves of NH_4^+ and NO_3^- S-ISM sensors from 50 to 1600 mg N/L. Comparison

between a millimeter-sized temperature solid-state sensor and a commercial nitrogen sensor under temperature shocks. Intercept of calibration curves for five pieces of nitrogen S-ISM sensors. Comparison of nitrogen S-ISM sensors with commercial sensors at five different concentrations (5, 10, 15, 20, and 25 mg-N/L). Resolution test of nitrogen S-ISM sensors at low (5 mg-N/L) and high (35 mg-N/L) concentrations. Selectivity tests of the nitrogen S-ISM sensors: shock tests using interference ions (added the ions simultaneously) and targeted ions for the nitrogen S-ISM sensors. The S-ISM on the working electrode of a NO₃⁻ S-ISM sensor after submerged in real wastewater for 7 d. The comparison of sensitivities of NH₄⁺ S-ISM sensors with the PVC ration of 33.3% and 40%. The pH interference at 20 mg N/L for nitrogen S-ISM sensors. Schematic diagram of data drifting on the surface of an NH₄⁺ S-ISM sensor. Alleviation of data drifting using an NH₄⁺ S-ISM_{CNT} sensor. Comparison of a WWTP with wireless nitrogen sensing technology capable of real-time control and adjustment and the one without wireless nitrogen sensing technology. Comparison of energy consumption and nitrogen discharge in a wastewater treatment plant (WWTP) with and without wireless nitrogen sensing technology. The cost analysis for S-ISM and commercial nitrogen sensors. (PDF)

AUTHOR INFORMATION

Corresponding Author

*E-mail: baikun.li@uconn.edu; Phone: 860-486-2339.

ORCID ®

Yu Lei: 0000-0002-0184-0373

Christian Brückner: 0000-0002-1560-7345

Baikun Li: 0000-0002-5623-5912

Notes

The authors declare no competing financial interest.

ACKNOWLEDGMENTS

This study was supported by National Science Foundation (NSF) Environmental Engineering Program GOALI Project (Grant No. 1706343), NSF Partnerships for Innovation, Accelerate Innovative Research Project (Grant No. 1640701), and Environmental Protection Agency Nitrogen Sensor Challenge Project (Grant No. OWSEPTICSYS 171400). The project is also partially funded by Infiltrator Water Technologies LLC. Y.H. is supported by the China Scholarship Council Doctorate Program. M.L. was supported by NSF Entrepreneur REU (E-REU) Program (hone institute: Dept. of Chemistry, Univ. of Alabama). The authors thank Pointwatch LLC. for kindly providing the circuit board and wireless gateway and Massachusetts Alternative Septic System Test Center for the great assistances during the 7 d field tests.

REFERENCES

- (1) McCarty, P. L. What is the Best Biological Process for Nitrogen Removal-When and Why? *Environ. Sci. Technol.* **2018**, *52* (7), 3835–3841.
- (2) Holmes, R. M.; McClelland, J. W.; Sigman, D. M.; Fry, B.; Peterson, B. J. Measuring $15N-NH_4^+$ in marine, estuarine and fresh waters: an adaptation of the ammonia diffusion method for samples with low ammonium concentrations. *Mar. Chem.* **1998**, *60* (3–4), 235-243.

- (3) Huber, S. A.; Balz, A.; Abert, M.; Pronk, W. Characterisation of aquatic humic and non-humic matter with size-exclusion chromatography—organic carbon detection—organic nitrogen detection (LC-OCD-OND). *Water Res.* **2011**, *45* (2), 879—885.
- (4) Moorcroft, M. J.; Davis, J.; Compton, R. G. Detection and determination of nitrate and nitrite: a review. *Talanta* **2001**, *54* (5), 785–803.
- (5) Ahmad, R.; Tripathy, N.; Khan, M. Y.; Bhat, K. S.; Ahn, M. S.; Hahn, Y. B. Ammonium ion detection in solution using vertically grown ZnO nanorod based field-effect transistor. *RSC Adv.* **2016**, 6 (60), 54836–54840.
- (6) Mahmoudian, M. R.; Alias, Y.; Basirun, W. J.; MengWoi, P.; Jamali-Sheini, F.; Sookhakian, M.; Silakhori, M. A sensitive electrochemical nitrate sensor based on polypyrrole coated palladium nanoclusters. *J. Electroanal. Chem.* **2015**, *751*, 30–36.
- (7) Crespo, G. A. Recent Advances in Ion-selective membrane electrodes for in situ environmental water analysis. *Electrochim. Acta* **2017**, 245, 1023–1034.
- (8) Seifert, T.; Sowade, E.; Roscher, F.; Wiemer, M.; Gessner, T.; Baumann, R. R. Additive manufacturing technologies compared: morphology of deposits of silver ink using inkjet and aerosol jet printing. *Ind. Eng. Chem. Res.* **2015**, *54* (2), 769–779.
- (9) Delannoy, P. E.; Riou, B.; Lestriez, B.; Guyomard, D.; Brousse, T.; Le Bideau, J. Toward fast and cost-effective ink-jet printing of solid electrolyte for lithium microbatteries. *J. Power Sources* **2015**, 274, 1085–1090.
- (10) Xu, Z.; Zhou, W.; Dong, Q.; Li, Y.; Cai, D.; Lei, Y.; Li, B.; et al. Flat flexible thin milli-electrode array for real-time in situ water quality monitoring in distribution systems. *Environ. Sci: Water Res. Technol.* **2017**, 3 (5), 865–874.
- (11) Xu, Z.; Dong, Q.; Otieno, B.; Liu, Y.; Williams, I.; Cai, D.; Li, B.; et al. Real-time in situ sensing of multiple water quality related parameters using micro-electrode array (MEA) fabricated by inkjet-printing technology (IPT). Sens. Actuators, B 2016, 237, 1108–1119.
- (12) Castellet, L.; Molinos-Senante, M. Efficiency assessment of wastewater treatment plants: A data envelopment analysis approach integrating technical, economic, and environmental issues. *J. Environ. Manage.* **2016**, *167*, 160–166.
- (13) Liu, B.; Lei, Y.; Li, B. A batch-mode cube microbial fuel cell based "shock" biosensor for wastewater quality monitoring. *Biosens. Bioelectron.* **2014**, *62*, 308–314.
- (14) Zakaria, Y.; Michael, K. An Integrated Cloud-Based Wireless Sensor Network for Monitoring Industrial Wastewater Discharged into Water Sources. WSN. 2017, 9 (08), 290–301.
- (15) Adu-Manu, K. S.; Tapparello, C.; Heinzelman, W.; Katsriku, F. A.; Abdulai, J. D. Water quality monitoring using wireless sensor networks: Current trends and future research directions. *ACM Trans. Sens. Netw.* **2017**, *13* (1), 4.
- (16) Dong, J.; Wang, G.; Yan, H.; Xu, J.; Zhang, X. A survey of smart water quality monitoring system. *Environ. Sci. Pollut. Res.* **2015**, 22 (7), 4893–4906.
- (17) Jensen, G. C.; Krause, C. E.; Sotzing, G. A.; Rusling, J. F. Inkjet-printed gold nanoparticle electrochemical arrays on plastic. Application to immunodetection of a cancer biomarker protein. *Phys. Chem. Chem. Phys.* **2011**, *13* (11), 4888–4894.
- (18) Saha, K.; Agasti, S. S.; Kim, C.; Li, X.; Rotello, V. M. Gold nanoparticles in chemical and biological sensing. *Chem. Rev.* **2012**, 112 (5), 2739–2779.
- (19) Ibanez, F. J.; Zamborini, F. P. Chemiresistive Sensing of Volatile Organic Compounds with Films of Surfactant-Stabilized Gold and Gold—Silver Alloy Nanoparticles. *ACS Nano* **2008**, 2 (8), 1543—1552
- (20) Garcia, C. A. B.; Júnior, L. R.; de Oliveira Neto, G. Determination of potassium ions in pharmaceutical samples by FIA using a potentiometric electrode based on ionophore nonactin occluded in EVA membrane. *J. Pharm. Biomed. Anal.* **2003**, *31* (1), 11–18.
- (21) Wroblewski, W.; Wojciechowski, K.; Dybko, A.; Brzózka, Z.; Egberink, R. J.; Snellink-Ruël, B. H.; Reinhoudt, D. N. Uranyl

- salophenes as ionophores for phosphate-selective electrodes. Sens. Actuators, B 2000, 68 (1-3), 313-318.
- (22) Zahran, E. M.; New, A.; Gavalas, V.; Bachas, L. G. Polymeric plasticizer extends the lifetime of PVC-membrane ion-selective electrodes. *Analyst* **2014**, *139* (4), 757–763.
- (23) Ahmadzadeh, S.; Rezayi, M.; Faghih-Mirzaei, E.; Yoosefian, M.; Kassim, A. Highly selective detection of titanium (III) in industrial waste water samples using meso-octamethylcalix [4] pyrrole-doped PVC membrane ion-selective electrode. *Electrochim. Acta* **2015**, *178*, 580–589.
- (24) Van Wie, B. J.; Li, X. Dual ionophore ion selective electrode for detecting non-ionic molecules, macromolecules and cells: *U.S. Patent Application*. 15/400, 528. 2017.
- (25) Gao, W.; Emaminejad, S.; Nyein, H. Y. Y.; Challa, S.; Chen, K.; Peck, A.; Lien, D. H.; et al. Fully integrated wearable sensor arrays for multiplexed in situ perspiration analysis. *Nature* **2016**, *529* (7587), 509–514.
- (26) Suzuki, K.; Siswanta, D.; Otsuka, T.; Amano, T.; Ikeda, T.; Hisamoto, H.; Ohba, S.; et al. Design and synthesis of a more highly selective ammonium ionophore than nonactin and its application as an ion-sensing component for an ion-selective electrode. *Anal. Chem.* **2000**, 72 (10), 2200–2205.
- (27) Chin, J.; Oh, J.; Jon, S. Y.; Park, S. H.; Walsdorff, C.; Stranix, B.; Kim, K.; et al. Tuning and dissecting electronic and steric effects in ammonium receptors: Nonactin vs artificial receptors. *J. Am. Chem. Soc.* **2002**, *124* (19), 5374–5379.
- (28) Beer, P. D.; Gale, P. A. Anion recognition and sensing: the state of the art and future perspectives. *Angew. Chem., Int. Ed.* **2001**, *40* (3), 486–516.
- (29) Singh, A. S.; Sun, S. S. Recognition, encapsulation, and selective fluorescence sensing of nitrate anion by neutral C 3-symmetric tripodal podands bearing amide functionality. *J. Org. Chem.* **2012**, 77 (4), 1880–1890.
- (30) Bühlmann, P.; Pretsch, E.; Bakker, E. Carrier-based ionselective electrodes and bulk optodes. 2. Ionophores for potentiometric and optical sensors. *Chem. Rev.* **1998**, *98* (4), 1593–1688.
- (31) Bakker, E.; Bühlmann, P.; Pretsch, E. Carrier-based ion-selective electrodes and bulk optodes. 1. General characteristics. *Chem. Rev.* **1997**, 97 (8), 3083–3132.
- (32) Kouba, V.; Vejmelkova, D.; Proksova, E.; Wiesinger, H.; Concha, M.; Dolejs, P.; Bartacek, J.; et al. High-rate partial nitritation of municipal wastewater after psychrophilic anaerobic pretreatment. *Environ. Sci. Technol.* **2017**, *51* (19), 11029–11038.
- (33) Yang, Q.; Peng, Y.; Liu, X.; Zeng, W.; Mino, T.; Satoh, H. Nitrogen removal via nitrite from municipal wastewater at low temperatures using real-time control to optimize nitrifying communities. *Environ. Sci. Technol.* **2007**, *41* (23), 8159–8164.
- (34) Guinovart, T.; Bandodkar, A. J.; Windmiller, J. R.; Andrade, F. J.; Wang, J. A potentiometric tattoo sensor for monitoring ammonium in sweat. *Analyst* **2013**, *138* (22), *7031*–*7038*.
- (35) Alizadeh, N.; Nabavi, S. Synthesis and characterization of novel tetra cyclo [4] pyrrole ether as an anion recognition element for nanocomposite nitrate ion selective carbon paste electrode. *Sens. Actuators, B* **2014**, 205, 127–135.
- (36) Bobacka, J. Potential stability of all-solid-state ion-selective electrodes using conducting polymers as ion-to-electron transducers. *Anal. Chem.* **1999**, *71* (21), 4932–4937.
- (37) (a) Rius-Ruiz, F. X.; Crespo, G. A.; Bejarano-Nosas, D.; Blondeau, P.; Riu, J.; Rius, F. X. Potentiometric strip cell based on carbon nanotubes as transducer layer: toward low-cost decentralized measurements. *Anal. Chem.* **2011**, *83* (22), 8810–8815. (b) Cranny, A. W. J.; Atkinson, J. K. Thick Film silver-silver chloride reference electrodes. *Meas. Sci. Technol.* **1998**, *9* (9), 1557–1565.
- (38) Polk, B. J.; Stelzenmuller, A.; Mijares, G.; MacCrehan, W.; Gaitan, M. Ag/AgCl microelectrodes with improved stability for microfluidics. *Sens. Actuators, B* **2006**, *114* (1), 239–247.
- (39) Rajkumar, D.; Song, B. J.; Kim, J. G. Electrochemical degradation of Reactive Blue 19 in chloride medium for the treatment

- of textile dyeing wastewater with identification of intermediate compounds. *Dyes Pigm.* **2007**, 72 (1), 1–7.
- (40) Ruch, P. W.; Čericola, D.; Hahn, M.; Kötz, R.; Wokaun, A. On the use of activated carbon as a quasi-reference electrode in non-aqueous electrolyte solutions. *J. Electroanal. Chem.* **2009**, *636* (1–2), 128–131.
- (41) Lee, J.; Jäckel, N.; Kim, D.; Widmaier, M.; Sathyamoorthi, S.; Srimuk, P.; Presser, V.; et al. Porous carbon as a quasi-reference electrode in aqueous electrolytes. *Electrochim. Acta* **2016**, 222, 1800–1805
- (42) Lundin, M.; Bengtsson, M.; Molander, S. Life cycle assessment of wastewater systems: influence of system boundaries and scale on calculated environmental loads. *Environ. Sci. Technol.* **2000**, 34 (1), 180–186.
- (43) Schazmann, B.; Morris, D.; Slater, C.; Beirne, S.; Fay, C.; Reuveny, R.; Diamond, D.; et al. A wearable electrochemical sensor for the real-time measurement of sweat sodium concentration. *Anal. Methods* **2010**, 2 (4), 342–348.
- (44) Jović, M.; Cortés-Salazar, F.; Lesch, A.; Amstutz, V.; Bi, H.; Girault, H. H. Electrochemical detection of free chlorine at inkjet printed silver electrodes. *J. Electroanal. Chem.* **2015**, *756*, 171–178.
- (45) Lian, L.; Yao, B.; Hou, S.; Fang, J.; Yan, S.; Song, W. Kinetic study of hydroxyl and sulfate radical-mediated oxidation of pharmaceuticals in wastewater effluents. *Environ. Sci. Technol.* **2017**, *51* (5), 2954–2962.
- (46) Barrera, E. L.; Spanjers, H.; Solon, K.; Amerlinck, Y.; Nopens, I.; Dewulf, J. Modeling the anaerobic digestion of cane-molasses vinasse: extension of the Anaerobic Digestion Model No. 1 (ADM1) with sulfate reduction for a very high strength and sulfate rich wastewater. *Water Res.* 2015, 71, 42–54.
- (47) Lei, Y.; Song, B.; van der Weijden, R. D.; Saakes, M.; Buisman, C. J. Electrochemical induced calcium phosphate precipitation: importance of local pH. *Environ. Sci. Technol.* **2017**, *51* (19), 11156–11164.
- (48) Yang, Q.; Peng, Y.; Liu, X.; Zeng, W.; Mino, T.; Satoh, H. Nitrogen removal via nitrite from municipal wastewater at low temperatures using real-time control to optimize nitrifying communities. *Environ. Sci. Technol.* **2007**, *41* (23), 8159–8164.
- (49) Michalska, A.; Maksymiuk, K. All-plastic, disposable, low detection limit ion-selective electrodes. *Anal. Chim. Acta* **2004**, 523 (1), 97–105.
- (50) Zamani, H. A.; Ganjali, M. R.; Behmadi, H.; Behnajady, M. A. Fabrication of an iron (III) PVC-membrane sensor based on bisbenzilthiocarbohydrazide as a selective sensing material. *Mater. Sci. Eng., C* **2009**, *29* (5), 1535–1539.
- (51) Zamani, H. A.; Ganjali, M. R.; Norouzi, P.; Tadjarodi, A.; Shahsavani, E. Determination of terbium (III) ions in phosphate rock samples by a Tb³⁺–PVC membrane sensor based on N, N-Dimethyl-N', N "-bis (4-methoxyphenyl) phosphoramidate. *Mater. Sci. Eng., C* **2008**, 28 (8), 1489–1494.
- (52) Manica, D. P.; Mitsumori, Y.; Ewing, A. G. Characterization of electrode fouling and surface regeneration for a platinum electrode on an electrophoresis microchip. *Anal. Chem.* **2003**, *75* (17), 4572–4577.
- (53) Vazquez, M.; Danielsson, P.; Bobacka, J.; Lewenstam, A.; Ivaska, A. Solution-cast films of poly (3, 4-ethylenedioxythiophene) as ion-to-electron transducers in all-solid-state ion-selective electrodes. *Sens. Actuators, B* **2004**, *97* (2–3), 182–189.
- (54) Gupta, V. K.; Singh, L. P.; Singh, R.; Upadhyay, N.; Kaur, S. P.; Sethi, B. A novel copper (II) selective sensor based on dimethyl 4, 4'(o-phenylene) bis (3-thioallophanate) in PVC matrix. *J. Mol. Liq.* **2012**, *174*, 11–16.
- (55) Fibbioli, M.; Morf, W. E.; Badertscher, M.; de Rooij, N. F.; Pretsch, E. Potential drifts of solid contacted ion selective electrodes due to zero current ion fluxes through the sensor membrane. *Electroanalysis* **2000**, *12* (16), 1286–1292.
- (56) Zhu, J.; Qin, Y.; Zhang, Y. Preparation of all solid-state potentiometric ion sensors with polymer-CNT composites. *Electro-chem. Commun.* **2009**, *11* (8), 1684–1687.

- (57) Crespo, G. A.; Macho, S.; Rius, F. X. Ion-selective electrodes using carbon nanotubes as ion-to-electron transducers. *Anal. Chem.* **2008**, *80* (4), 1316–1322.
- (58) Sundfors, F.; Lindfors, T.; Höfler, L.; Bereczki, R.; Gyurcsányi, R. E. FTIR-ATR study of water uptake and diffusion through ion-selective membranes based on poly (acrylates) and silicone rubber. *Anal. Chem.* **2009**, *81* (14), 5925–5934.
- (59) Sundfors, F.; Höfler, L.; Gyurcsányi, R. E.; Lindfors, T. Influence of Poly (3 octylthiophene) on the Water Transport Through Methacrylic Acrylic Based Polymer Membranes. *Electroanalysis* **2011**, 23 (8), 1769–1772.
- (60) Hu, J.; Zou, X. U.; Stein, A.; Bühlmann, P. Ion-selective electrodes with colloid-imprinted mesoporous carbon as solid contact. *Anal. Chem.* **2014**, *86* (14), 7111–7118.